IEEE Access
Multidisciplinary ⋮ Rapid Review ⋮ Open Access Journal

Received 22 July 2025, accepted 28 August 2025, date of publication 9 September 2025, date of current version 22 September 2025.

Digital Object Identifier 10.1109/ACCESS.2025.3608012

RESEARCH ARTICLE

A Slow-Light Mach-Zehnder Interferometric Switch With One-Dimensional Grating Waveguides

HONG GAO, FUJUN SUN, GANG YANG, TIANYANG FU, ZAILI YANG, JING XIAO, WEI TANG, AND YAN YANG

Key Laboratory of Fabrication Technologies for Integrated Circuits, Chinese Academy of Sciences, Beijing 100029, China
Institute of Microelectronics, Chinese Academy of Sciences, Beijing 100029, China
School of Integrated Circuits, University of Chinese Academy of Sciences, Beijing 100049, China

Corresponding authors: Yan Yang (yyang10@ime.ac.cn) and Fujun Sun (sunfujun@ime.ac.cn)

This work was supported in part by the National Key Research and Development Program of China under Grant 2022YFB2802400, in part by the National Natural Science Foundation of China under Grant 62274179 and Grant 62235001, in part by the 173 Technical Field Fund under Grant 2023-JCJQ-JJ-1017 and Grant 2022-JCJQ-JJ-0446, and in part by the International Partnership Program of Chinese Academy of Sciences under Grant 02GJHZ2023026FN.

ABSTRACT Optical switches are essential components of all-optical switching networks, enabling optical path switching in the optical domain without the need for electronic conversion. However, the design of optical switches with low-power and ultra-compact footprints remains a significant challenge. In this work, a slow-light thermo-optic (TO) Mach-Zehnder interferometer (MZI) switch based on one-dimensional (1D) grating waveguides is proposed. The proposed structure, with a compact footprint of 72 μm, exhibited both strong and weak slow-light regions. In the strong-slow-light region, the structure achieved a high group index (n_g) at a wavelength of 1539.8 nm, with a power consumption of 3.9 mW. Different from conventional designs that rely solely on strong-slow-light effects near the bandgap edge, our approach utilizes the weak-slow-light region centered around 1550 nm. This enables a broader operational bandwidth (∼109.5 nm) while maintaining a low switching power of 8.73 mW. The integrated structure presented in this work is promising for building ultra-compact and broadband photonic networks.

INDEX TERMS Optical switch, Mach-Zehnder interferometer, 1D grating waveguides, slow-light.

I. INTRODUCTION

Optical switch units are the fundamental building blocks of optical switching array chips. With the rapid growth of data traffic and increasing demand for high-capacity communication systems, optical switching arrays are being scaled up to accommodate larger port counts and higher integration densities. However, this trend introduces significant challenges in terms of power consumption and the footprint. Hence, there is an urgent need to develop compact and energy-efficient optical switch units to enable the large-scale deployment of next-generation optical switching chips in the field of silicon photonics.

Silicon-based optical switches are mainly categorized into three structural types: MZIs [1], microring resonators (MRRs) [2], and hybrid MRR-MZI configurations [3] MRRs feature compact footprints and intrinsic wavelength selectivity, but their performance is constrained by narrow bandwidth and high sensitivity to fabrication imperfections [4], [5] In contrast, MZIs offer broader optical bandwidth and higher fabrication tolerance, making them better suited for high-capacity communication systems [6], [7], [8], [9], MZI switches typically employ electro-optic (EO) or TO modulation. Among these, TO-MZI switches have gained widespread adoption owing to their low fabrication cost and excellent compatibility with standard CMOS processes. However, conventional TO-MZI switches require relatively long optical paths and high power consumption, limiting their suitability for compact and energy-efficient integration [10]

The associate editor coordinating the review of this manuscript and approving it for publication was Sukhdev Roy.

Low-power and compact TO-MZI switches can be achieved by enhancing the modulation efficiency of the phase-shifting arm or by reducing the refractive index change required for switching. Various efforts have been made to reduce the footprint and power consumption of TO-MZI switches. Approaches such as incorporating indium tin oxide (ITO) or other transparent conductive oxides have enabled compact devices, but often at the expense of higher insertion losses [11], [12], [13], In recent years, slow-light effects have been employed in optical switches to enhance phase modulation and strengthen light-matter interactions, thereby enabling significant reductions in power consumption [14] Slow-light waveguide structures can be divided into two main categories: two-dimensional photonic crystal (2D PhC) waveguides and one-dimensional (1D) PhC waveguides [15] The latter category includes typical structures such as Bragg gratings (BGs) [16] and subwavelength gratings (SWGs) [17], [18] 2D PhC waveguides exhibit strong-slow-light effects near the photonic bandgap edge and offer highly flexible dispersion engineering [19], [20] However, they often suffer from narrow bandwidths, high propagation losses [21], and complex fabrication processes, limiting their large-scale integration potential. In contrast, 1D PhC waveguides offer simpler fabrication and lower loss, making them more attractive for large-scale integration. However, the slow-light effect in 1D PhC structures is generally weaker than that in their 2D PhC, and the degrees of dispersion engineering and structural tunability are more limited due to their simpler geometry and fewer design parameters.

In this study, we employed a 1D "fishbone" grating waveguide on a silicon-on-insulator (SOI) platform, which introduces additional structural degrees of freedom beyond those of conventional 1D PhCs. This enhanced structural flexibility enables improved control of the dispersion characteristics. We investigate the impact of 1D grating waveguides on slow-light behavior. Our analysis reveals that, in addition to the conventional strong-slow-light region near the bandgap edge characterized by a rapidly varying n_g and narrow bandwidth, 1D grating waveguides also exhibit a weak-slow-light region, where n_g remains relatively stable across a much broader spectral range. By incorporating this weak-slow-light region into the TO-MZI switch, we achieve a compact device footprint of only 72 μm with a switching power of 8.73 mW. Moreover, the grating waveguide maintained a wide operational bandwidth of 109.5 nm with a relatively low insertion loss. These results highlight the potential of weak-slow-light engineering in 1D grating waveguides for the realization of energy-efficient, broadband, and compact photonic switches, paving the way for the construction of ultra-compact and high-performance photonic integrated networks.

II. DESIGN AND THEORY

A. STRUCTURE DESIGN

A schematic of the designed TO-MZI switch structure is shown in Fig. 1. The device consists of two 2 × 2 Multi-Mode Interferometer (MMI) couplers and two waveguide arms. At the input, the MMI coupler evenly splits the optical signal into two waveguide arms. After propagating through these arms, the phase-modulated optical signals are recombined at the output using a second MMI coupler. Both waveguide arms feature identical slow-light 1D "fishbone" structures, consisting of a backbone region and periodic "teeth" regions on both sides of the backbone along the x-direction. The fishbone waveguide structure is characterized by the backbone width (W_{strip}), teeth width (W_{wg}), teeth period (Λ), and teeth length ($\Lambda \cdot f$), where f is the duty cycle of the 1D grating waveguides.

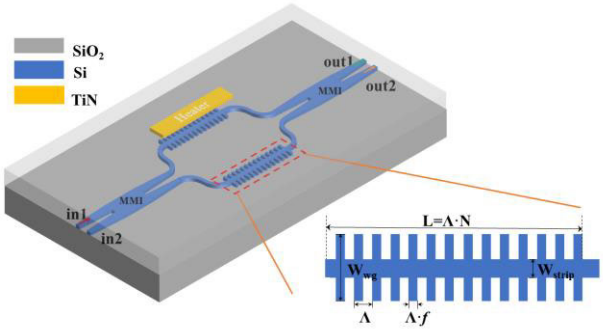

FIGURE 1. Schematic of MZI switch structure based on slow-light 1D grating waveguide.

A titanium nitride (TiN) microheater was integrated onto one of the waveguide arms. The distance between the TiN microheater and the waveguide is 1 μm, following the design rules of the silicon photonics multi-project wafer (MPW) platform provided by the Institute of Microelectronics of the Chinese Academy of Sciences (IMECAS). In principle, reducing the vertical separation can improve the heating efficiency, shorten the response time, and lower the power consumption, but it also exacerbates thermal crosstalk and increases optical absorption loss. In this study, the chosen distance provided a balance between thermal efficiency and optical performance. The heater utilizes the TO effect to modulate the effective refractive index (n_{eff}) of the waveguide arm, thereby enabling phase modulation. When the phase difference between the two waveguide arms is 0, the switch is in the "cross" state, meaning that light entering from in1 (or in2) exits through out2 (or out1) When the phase difference between the two waveguide arms is π, the switch is in the "bar" state, and the light entering from in1(or in2) exits through out1(or out2).

B. PRINCIPLE

1) THERMO-OPTIC EFFECT

The TO switch generates a phase shift $\Delta\varphi$ based on the TO effect, which can be obtained by [22]:

$$\Delta\varphi = \frac{2\pi}{\lambda} \cdot \frac{dn_{eff}}{dT} \Delta T \cdot L \tag{1}$$

where λ is the wavelength, $\frac{dn_{eff}}{dT}$ is the temperature coefficient of the effective refractive index, L is the heat conduction path, and ΔT is the temperature variation. Here, $\frac{dn_{eff}}{dT}$ is determined

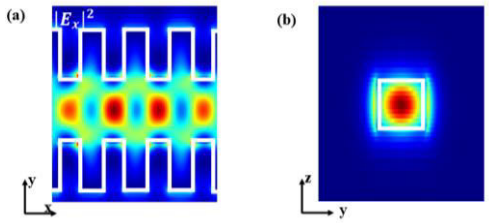

FIGURE 2. (a) Distribution of the electric field on the xy plane. (b) Distribution of the electric field on the yz plane.

not only by the intrinsic properties of the material but also by the structural design of the waveguide and the confinement of the optical mode A higher $\frac{dn_{eff}}{dT}$ indicates a stronger sensitivity of the refractive index of the waveguide to temperature changes, which is critical for efficient phase modulation. For the TO switches, ΔT was proportional to the thermal power (P_{heat}) applied by the TiN heater. Therefore, it can be inferred that the design of TO switches requires careful consideration of the material properties, waveguide geometry, and heating efficiency to achieve optimal performance with minimal power consumption.

2) SLOW LIGHT EFFECTS IN 1D GRATING WAVEGUIDES

The 1D ''fishbone'' waveguide is a type of optical waveguide characterized by a periodic arrangement of high-low refractive-index materials, where Λ is much smaller than the operating wavelength (λ). The transmission characteristics of the periodic fishbone structure can be described using the Bloch theorem The field distribution of the TE_0mode is shown in Fig. 2. The propagation of optical signals is mainly confined to the backbone, whereas the grating teeth serve as the supporting modulators.

1D grating waveguides can achieve optical dispersion control by adjusting the grating structure parameters. The critical structural parameters of 1D grating waveguides include Λ, duty cycle f, W_{strip}, and W_{wg} Through optical dispersion design, the group velocity (v_g) of light within a waveguide can be significantly reduced, thus realizing a slow-light effect.. The v_g and n_g of light transmitted in waveguides can be expressed as [23], [24]:

$$vg = \frac{d\omega}{dk} = \frac{d(2\pi f)}{d(kx \cdot \frac{2\pi}{\Lambda})} \tag{2}$$

$$ng = \frac{c}{vg} \tag{3}$$

where f represents the frequency, ω is the angular frequency, Λ is the period length, k is the wave vector, and $k_x$is the normalized wave vector. For the same change in angular frequency ($\Delta\omega$), dispersion analysis revealed that the Δk in the slow-light region was larger than that in the fast-light region. Then, according to (2), a low $v_g$can be achieved, which increases the light-thermal interaction time. Consequently, a high n_g can be achieved, which can effectively amplify the phase change of an optical signal

A slow-light waveguide regulates the dispersion characteristics of light waves by periodically modulating the refractive index distribution of the waveguide. The effective refractive index change (Δn_{eff}) induced by the slow-light waveguide under a certain temperature change can be derived based on the principles discussed in [19] and [25], and is expressed as:

$$\Delta n_{eff} = a \cdot \Delta T \cdot \Gamma \cdot n_g / n_{Si} \tag{4}$$

where a is the TO coefficient of silicon, ΔT is the temperature increase caused by the heater, $\Gamma \equiv \frac{<E|\varepsilon|E>_d}{<E|\varepsilon|E>_a}$ is the filling fraction defining the fraction of the optical field confined in silicon, $n_g$is the group index of the slow-light waveguide, and n_{Si} is the refractive index of silicon. The phase shift required to switch between the two states of the optical switch was fixed. According to (1) and (4), when $\Delta\varphi$ is constant, n_g is inversely proportional to $L$and ΔT Here, L is related to the number of grating periods (N). ΔT was proportional to the P_{heat} of the heater. Therefore, in regions with a strong-slow-light effect, where $n_g$is large, the $P_{heat}$of the MZI optical switch can be effectively reduced, while also enabling further miniaturization of the physical size of the device

III. SIMULATION AND OPTIMIZATION

A. WAVEGUIDE STRUCTURE DESIGN

The slow-light effect was primarily achieved by controlling the dispersion relations By optimizing the structural parameters, such as W_{wg}, Λ, and duty cycle f, the dispersion of the grating can be effectively controlled, thereby realizing the desired slow-light effect. To evaluate this effect, three-dimensional finite-difference time-domain (3D-FDTD) simulations were performed to analyze the influence of different structural parameters on the slow-light effect of a 1D ''fishbone'' waveguide on the SOI platform. The dispersion relation was computed using Bloch boundary conditions, and n_g was extracted from the slope of the dispersion curve To further confirm the validity of this method, supplementary time-of-flight (TOF) analysis was performed, in which the group delay of a narrowband pulse propagating through the waveguide was measured and converted to n_g The consistency between the two methods confirms the reliability of the approach employed in this study.

Altering the W_{wg} can affect the boundary conditions of the modes, thereby changing their propagation characteristic. Fig. 3(a) shows the dispersion curves for different W_{wg} values increasing from 1.1 μm to 2.0 μm. Each dispersion curve had two regions with relatively gentle slopes. The corresponding n_g values for different W_{wg} are shown in Fig. 3(b). The curve shows a ''U-shaped'' trend, with a high n_g on both sides, indicating a significant slow-light effect observed at longer and shorter wavelengths. As W_{wg} gradually increases, the slow-light region on the left exhibits a red shift and reduction in the operational bandwidth In the middle part of the ''U-shaped'' curve, n_g is relatively small and stable. As W_{wg} increases, n_g in the middle part also increases, which further enhances the slow-light effect in this region.

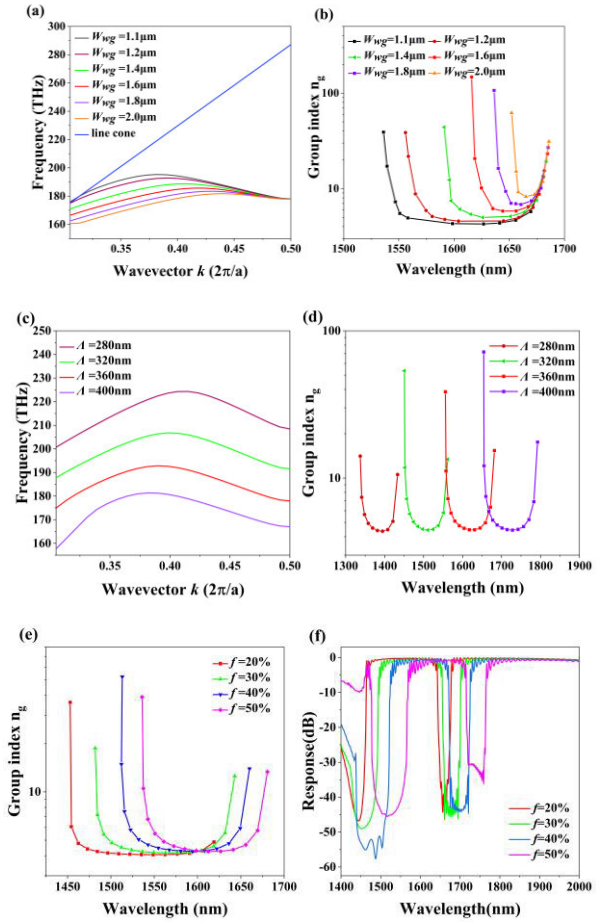

FIGURE 3. (a) Dispersion profiles of the guided mode for various teeth width (W_{wg}). (b) Group refractive index for various teeth width (W_{wg}). (c) Dispersion profiles of the guided mode for various period lengths(Λ). (d) Group refractive index of various period lengths(Λ). (e) Group refractive index for various duty cycles f. (f) Spectral response of different duty cycles f.

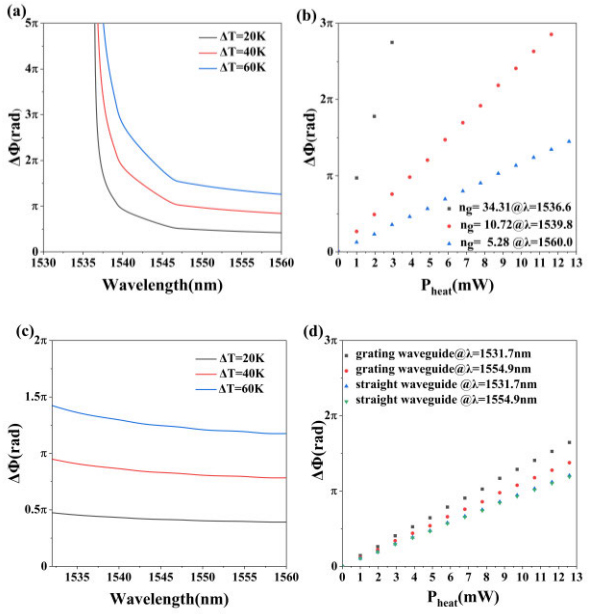

FIGURE 4. (a) Phase shift for different temperature under strong-slow-light effect. (b) Phase shift and different heat power for group index under strong-slow-light effect. (c) Phase shift for different temperature variations under weak-slow-light effect. (d) Phase shift and different heat power for different wavelengths under weak-slow-light effect.

The variation in Λ influences the size of the Brillouin zone and, thereby, the energy band structure. In Fig. 3(c), when $W_{wg} = 1.2\ \mu$m is constant, and Λ increases from 280 nm to 400 nm, the dispersion curve shifts integrally towards the low-frequency direction (red shift). Fig. 3(d) presents the variation of n_g with the wavelength, and the curve exhibits a ''U-shaped'' feature, that is, n_g is higher in the short-wave and long-wave regions but lower in the middle-wave band. As Λ increased, the n_g curve shifted integrally towards the long-wavelength direction, which is in accordance with the movement trend of the dispersion curve. A smaller Λ has a greater effect on optical waves of shorter wavelengths, whereas a larger Λ has a greater effect on optical waves of longer wavelengths. By fixing W_{strip} =450 nm, $W_{wg} = 1.1\ \mu$m, and $\Lambda = 360$ nm, the influence of the duty cycle $f$on the slow-light characteristics of the slow-light waveguide is illustrated in Fig. 3(e). Fig. 3(f) shows the spectral response of different duty cycles f, where a blue shift occurs as the duty cycle decreases The change in the duty cycle affects the n_{eff} of the slow-light waveguide, and the change in n_{eff} directly affects n_g Moreover, as shown in Fig. 3(f), it can be observed that pronounced sideband oscillations appear near the photonic band edge in the strong-slow-light region, where the n_g increases sharply. In contrast, the weak-slow-light region exhibits a much smoother and more stable transmission response.

B. SIMULATION VERIFICATION OF SLOW-LIGHT PHASE SHIFT

Typically, the relationship curve between n_g and the wavelength of the slow-light waveguide presents a ''U-shaped'', corresponding to the slow-light regions with sharp changes in n_g on both sides of the curve and the slow-light region with a gentle change at the bottom of the U-shaped The n_g changes sharply on both sides, resulting in extremely narrow bandwidths and group velocity dispersion (GVD) [26], which leads to significant signal distortion. Based on the calculations from (1) and (4), the length of the 1D slow-light waveguide was determined to be L= 72 μm. Fig. 4(a) shows the phase variation corresponding to different modulation temperatures under the strong-slow-light effect in the wavelength range of 1530-1560 nm for a slow-light waveguide with structural dimensions: $W_{wg} = 1.1\ \mu$m, Λ = 036 μm, $W_{\text{strip}} = 045\ \mu$m, and duty cycle f= 50%. Fig. 4(b) shows the relationship between the phase shift and P_{heat} for three different n_g value$_s$: 34.31, 1072, and 5.28 The larger the n_g, the smaller the P_{heat} required to achieve a phase shift of π At a group index n_g of 1072 with a corresponding wavelength of 1539.8 nm, the P_π is 3.9 mW. Furthermore, when allowing a $\pm$10% fluctuation around this central n_g =1072, the bandwidth of the strong-slow-light region was determined to be 1.1 nm.

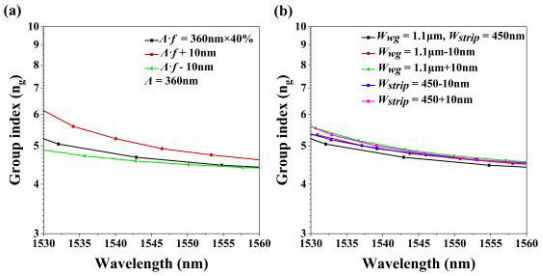

FIGURE 5. (a) Group index variation with wavelength for slow-light waveguide under ±10 nm $\Lambda \cdot f$ variation; (b) Group index variation with wavelength for slow-light waveguide under ±10 nm W_{wg} and W_{strip} variation.

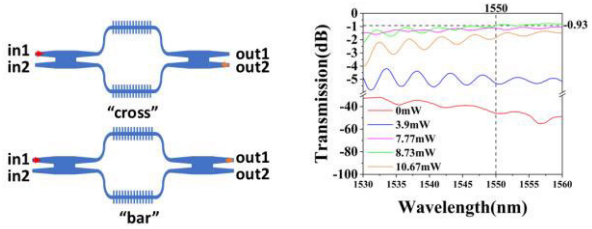

FIGURE 6. Transmission characteristic curves for the output 1 under different power levels.

Fig. 4(c) shows the phase variation corresponding to different modulation temperatures in the region where the slow-light effect is more stable within the wavelength range of 1530-1560 nm. According to the expected working band (C-band), a structure with a duty cycle of $f = 40\%$, $W_{strip} = 450$ nm, $W_{wg} = 1.1$ μm, and $\Lambda = 360$ nm was selected. In comparison with the region of the strong-slow-light effect, Fig. 4(c) shows the region with a more stable $\Delta\varphi$ Although the required P_{heat} in the weak-slow-light region is slightly higher than that in the strong-slow-light region near the band edge, Fig. 4(d) demonstrates that employing the weak-slow-light region in the slow-light waveguide phase shifter still results in a lower P_{heat} than that of a conventional straight waveguide. Fig. 4(d) shows the dependence of the TO phase shift on P_{heat} for two distinct wavelengths 1531.7 nm ($n_g = 5.08$) and 1554.9 nm ($n_g = 4.56$).

Lithography and etching are key processes that determine the accuracy of feature dimensions in the fabrication of silicon-based photonic devices The device structure proposed in this study is fully compatible with fabrication using a 130 nm silicon photonics process node. Since slow-light devices are particularly sensitive to dimensional variations, especially in periodic grating structures, where even minor deviations can significantly affect the group index and bandwidth, we systematically evaluated the impact of process-induced variations in critical dimensions on device performance. As shown by the black curve in Fig. 5, the n_g at the center wavelength of the C-band was approximately 4.7. Furthermore, considering a ±10% fluctuation around $n_g = 4.7$, the bandwidth of the weak-slow-light region was determined to be 109.5 nm. Fig. 5(a) illustrates the influence of ±10 nm fabrication tolerance in the $\Lambda \cdot f$ on the slow-light characteristics of the slow-light waveguide. When $\Lambda \cdot f$ is varied by ±10 nm, the n_g variation across the C-band remains within 15%. Fig. 5(b) shows the influence of ±10 nm fabrication tolerance in W_{wg} and W_{strip} on the slow-light characteristics of the slow-light waveguide. The results exhibited only minor variations in n_g, indicating a high tolerance to fabrication deviations.

C. DESIGN OF 2 × 2 OPTICAL SWITCH

To balance power reduction and device miniaturization without significantly compromising the bandwidth, the weak-slow-light region with a flat n_g near the "U-shaped" bottom is utilized in the TO-MZI switch. Fig. 6 illustrates the transmission spectra at the out1 port of the TO-MZI switch when light is injected from in1 and the slow-light waveguide phase arm is modulated at different P_{heat} values As a design example, for a 72 μm long slow-light waveguide, the required P_{heat} to achieve a switching state at a wavelength of 1550 nm is approximately 8.73 mW, corresponding to a transmission loss of −0.93 dB.

IV. DISCUSSION

To make a clear comparison, the performance of the TO-MZI structure obtained in this study and those in some previously published papers [27], [28], [29], are presented in Table 1. In [27], an asymmetrically doped MMI phase shifter combined with an integrated metal heat sink enabled a highly compact and ultrafast TO-MZI switch, but with moderately increased power consumption and fabrication complexity. In [28], a polarization-insensitive switch was realized by employing square-cross-section waveguides to equalize the TO coefficients for TE and TM modes, but the significantly reduced tuning efficiency of the 220 nm-wide waveguide led to high power consumption In [29], by utilizing a mode-looped multimode waveguide phase shifter, a broadband TO-MZI switch was demonstrated, covering the entire O–E–S–C–L–U bands with high extinction ratios, but with slightly higher power consumption, and a larger device footprint Compared with other types of waveguide designs, the silicon-based TO-MZI switch proposed in this study offers a simpler structure and lower power consumption, and can meet various application requirements by flexibly adjusting the structural parameters, demonstrating superior comprehensive performance.

The slow-light effect assists the TO switch and enhances the modulation efficiency of the optical switch. Furthermore, employing the weak-slow-light region in the TO-MZI switch results in a low insertion loss (<1 dB) This type of optical switch unit has great potential for implementation in large-scale array optical-switch chips. However, further reducing the power consumption by increasing the slow-light effect introduces challenges, such as increased loss, reduced bandwidth, and spectral ripples near the photonic band edge As a future challenge, introducing dispersion-engineered materials or designing chirped or apodized structures [30], [31] could help suppress these effects, improve spectral

TABLE 1. Comparison of performance between this study and other TO-MZI switches.

Year	Waveguide Structure	Simulated P_π (mW)	L (μm)
2021[27]	Multimode Waveguide (Asymmetrically Doped)	21	9.5
2022 [28]	Square-cross-section Waveguide	146.3	100
2024 [29]	Multimode straight Waveguide	11.58	100
This work (strong-slow-light)	1D "fishbone" grating waveguide	3.9	72
This work (weak-slow-light)		8.73	72

uniformity, and broaden the usable bandwidth, thereby further optimizing device performance.

V. CONCLUSION

This study proposes a TO-MZI switch based on the slow light effect By analyzing how the parameters of 1D slow-light waveguide affect n_g and bandwidth, an optimized slow-light waveguide is employed as a thermally modulated arm to realize a low-power and small-footprint TO switch. The results demonstrate that the TO-MZI switch based on slow-light effect can enhance modulation efficiency and reduce power consumption. Therefore, the TO-MZI switch with slow-light effect presented in this study, owing to its CMOS compatibility and compact footprint, exhibits inherent scalability that makes it well suited for constructing high-density optical switch arrays. Its broadband and low-power characteristics also make it a strong candidate for high-capacity all-optical interconnection networks, paving the way to realize large scale photonic integrated circuits.

REFERENCES

[1] N. Dupuis, B. G. Lee, A. V. Rylyakov, D. M. Kuchta, C. W. Baks, J. S. Orcutt, D. M. Gill, W. M. J. Green, and C. L. Schow, "Design and fabrication of low-insertion-loss and low-crosstalk broadband 2 × 2 Mach–Zehnder silicon photonic switches," *J. Lightw. Technol.*, vol. 33, no. 17, pp. 3597–3606, Jun. 17, 2015, doi: 10.1109/JLT.2015.2446463.

[2] S.-J. Chang, C.-Y. Ni, Z. Wang, and Y.-J. Chen, "A compact and low power consumption optical switch based on microrings," *IEEE Photon. Technol. Lett.*, vol. 20, no. 12, pp. 1021–1023, Jun. 30, 2008, doi: 10.1109/LPT.2008.923763.

[3] L. Lu, L. Zhou, X. Li, and J. Chen, "Low-power 2×2 silicon electro-optic switches based on double-ring assisted Mach–Zehnder interferometers," *Opt. Lett.*, vol. 39, no. 6, pp. 1633–1636, Mar. 2014, doi: 10.1364/ol.39.001633.

[4] P. Dong, S. F. Preble, and M. Lipson, "All-optical compact silicon comb switch," *Opt. Exp.*, vol. 15, no. 15, pp. 9600–9605, Jul. 2007, doi: 10.1364/oe.15.009600.

[5] A. Biberman, H. L. R. Lira, K. Padmaraju, N. Ophir, J. Chan, M. Lipson, and K. Bergman, "Broadband silicon photonic electrooptic switch for photonic interconnection networks," *IEEE Photon. Technol. Lett.*, vol. 23, no. 8, pp. 504–506, Feb. 10, 2011, doi: 10.1109/LPT.2011.2112763.

[6] F. Wang, J. Yang, L. Chen, X. Jiang, and M. Wang, "Optical switch based on multimode interference coupler," *IEEE Photon. Technol. Lett.*, vol. 18, no. 2, pp. 421–423, Jan. 31, 2006, doi: 10.1109/LPT.2005.863201.

[7] A. Densmore, S. Janz, R. Ma, J. H. Schmid, D.-X. Xu, A. Delâge, J. Lapointe, M. Vachon, and P. Cheben, "Compact and low power thermo-optic switch using folded silicon waveguides," *Opt. Exp.*, vol. 17, no. 13, pp. 10457–10465, Jun. 2009, doi: 10.1364/oe.17.010457.

[8] J. Van Campenhout, W. M. Green, S. Assefa, and Y. A. Vlasov, "Low-power, 2×2 silicon electro-optic switch with 110-nm bandwidth for broadband reconfigurable optical networks," *Opt. Exp.*, vol. 17, no. 26, pp. 24020–24029, Dec. 2009, doi: 10.1364/oe.17.024020.

[9] M. R. Watts, J. Sun, C. DeRose, D. C. Trotter, R. W. Young, and G. N. Nielson, "Adiabatic thermo-optic Mach–Zehnder switch," *Opt. Lett.*, vol. 38, no. 5, pp. 733–735, Mar. 2013, doi: 10.1364/ol.38.000733.

[10] Á. Rosa, A. Gutiérrez, A. Brimont, A. Griol, and P. Sanchis, "High performace silicon 2×2 optical switch based on a thermo-optically tunable multimode interference coupler and efficient electrodes," *Opt. Exp.*, vol. 24, no. 1, pp. 191–198, Jan. 2016, doi: 10.1364/oe.24.000191.

[11] R. Amin, R. Maiti, C. Carfano, Z. Ma, M. H. Tahersima, Y. Lilach, D. Ratnayake, H. Dalir, and V. J. Sorger, "0.52 V mm ITO-based Mach–Zehnder modulator in silicon photonics," *APL Photon.*, vol. 3, no. 12, Dec. 2018, Art. no. 126104, doi: 10.1063/1.5052635.

[12] E. Li, B. A. Nia, B. Zhou, and A. X. Wang, "Transparent conductive oxide-gated silicon microring with extreme resonance wavelength tunability," *Photon. Res.*, vol. 7, no. 4, pp. 473–477, Apr. 2019, doi: 10.1364/prj.7.000473.

[13] R. Amin, R. Maiti, Y. Gui, C. Suer, M. Miscuglio, E. Heidari, R. T. Chen, H. Dalir, and V. J. Sorger, "Sub-wavelength GHz-fast broadband ITO Mach–Zehnder modulator on silicon photonics," *Optica*, vol. 7, no. 4, pp. 333–335, Apr. 2020, doi: 10.1364/optica.389437.

[14] T. F. Krauss, "Why do we need slow light?" *Nature Photon.*, vol. 2, no. 8, pp. 448–450, Aug. 2008, doi: 10.1038/nphoton.2008.139.

[15] Z. Peng, Y. Huang, K. Zheng, C. Zheng, M. Pi, H. Zhao, J. Ji, Y. Min, L. Liang, F. Song, Y. Zhang, Y. Wang, and F. K. Tittel, "Slow-light-enhanced on-chip 1D and 2D photonic crystal waveguide gas sensing in near-IR with an ultrahigh interaction factor," *Photon. Res.*, vol. 11, no. 10, pp. 1647–1656, Oct. 2023, doi: 10.1364/prj.494762.

[16] A. Chen, M. Zhang, D. Crowley, N. Gangi, and Z. R. Huang, "Silicon photonics foundry fabricated, slow-light enhanced, low power thermal phase shifter," *J. Appl. Phys.*, vol. 136, no. 16, Oct. 2024, Art. no. 163101, doi: 10.1063/5.0219996.

[17] L. Torrijos-Morán, A. Brimont, A. Griol, P. Sanchis, and J. García-Rupérez, "Ultra-compact optical switches using slow light bimodal silicon waveguides," *J. Lightw. Technol.*, vol. 39, no. 11, pp. 3495–3501, Mar. 17, 2021, doi: 10.1109/JLT.2021.3066479.

[18] R. Halir, P. J. Bock, P. Cheben, A. Ortega-Moñux, C. Alonso-Ramos, J. H. Schmid, J. Lapointe, D.-X. Xu, J. G. Wangüemert-Pérez, Ì. Molina-Fernández, and S. Janz, "Waveguide sub-wavelength structures: A review of principles and applications," *Laser Photon. Rev.*, vol. 9, no. 1, pp. 25–49, Jan. 2015, doi: 10.1002/lpor.201400083.

[19] S. Yan, X. Zhu, L. H. Frandsen, S. Xiao, N. A. Mortensen, J. Dong, and Y. Ding, "Slow-light-enhanced energy efficiency for graphene microheaters on silicon photonic crystal waveguides," *Nature Commun.*, vol. 8, no. 1, p. 14411, Feb. 2017, doi: 10.1038/ncomms14411.

[20] T. Tamura, K. Kondo, Y. Terada, Y. Hinakura, N. Ishikura, and T. Baba, "Silica-clad silicon photonic crystal waveguides for wideband dispersion-free slow light," *J. Lightw. Technol.*, vol. 33, no. 14, pp. 3034–3040, Apr. 7, 2015, doi: 10.1109/JLT.2015.2420685.

[21] L. O'Faolain, T. P. White, D. O'Brien, X. Yuan, M. D. Settle, and T. F. Krauss, "Dependence of extrinsic loss on group velocity in photonic crystal waveguides," *Opt. Exp.*, vol. 15, no. 20, pp. 13129–13138, Oct. 2007, doi: 10.1364/oe.15.013129.

[22] S. Liu, J. Feng, Y. Tian, H. Zhao, L. Jin, B. Ouyang, J. Zhu, and J. Guo, "Thermo-optic phase shifters based on silicon-on-insulator platform: State-of-the-art and a review," *Frontiers Optoelectronics*, vol. 15, no. 1, p. 9, Dec. 2022, doi: 10.1007/s12200-022-00012-9.

[23] P. Jean, A. Gervais, S. LaRochelle, and W. Shi, "Slow light in sub-wavelength grating waveguides," *IEEE J. Sel. Topics Quantum Electron.*, vol. 26, no. 2, pp. 1–8, Mar. 2020, doi: 10.1109/JSTQE.2019.2933788.

[24] Y. Ma, B. Dong, B. Li, J. Wei, Y. Chang, C. P. Ho, and C. Lee, "Mid-infrared slow light engineering and tuning in 1-D grating waveguide," *IEEE J. Sel. Topics Quantum Electron.*, vol. 24, no. 6, pp. 1–8, Nov. 2018, doi: 10.1109/JSTQE.2018.2827659.

[25] J. Witzens, "High-speed silicon photonics modulators," *Proc. IEEE*, vol. 106, no. 12, pp. 2158–2182, Dec. 2018, doi: 10.1109/JPROC.2018.2877636.
[26] R. J. P. Engelen, Y. Sugimoto, Y. Watanabe, J. P. Korterik, N. Ikeda, N. F. van Hulst, K. Asakawa, and L. Kuipers, "The effect of higher-order dispersion on slow light propagation in photonic crystal waveguides," *Opt. Exp.*, vol. 14, no. 4, pp. 1658–1672, Mar. 2006, doi: 10.1364/oe.14.001658.
[27] T. Kita and M. Mendez-Astudillo, "Ultrafast silicon MZI optical switch with periodic electrodes and integrated heat sink," *J. Lightw. Technol.*, vol. 39, no. 15, pp. 5054–5060, May 21, 2021, doi: 10.1109/JLT.2021.3082634.
[28] W. Li, L. Xu, J. Zhang, D. Mao, Y. D'Mello, Z. Wei, and D. V. Plant, "Broadband polarization-insensitive thermo-optic switches on a 220-nm silicon-on-insulator platform," *IEEE Photon. J.*, vol. 14, no. 6, pp. 1–10, Dec. 2022, doi: 10.1109/JPHOT.2022.3218753.
[29] W. Li, L. Xu, D. Turgeon, Z. Wei, J. Zhang, C. St-Arnault, W. Shi, and D. V. Plant, "Power-efficient silicon photonic thermo-optic switch covering OESCLU-bands enabled by mode-looped phase shifters with subwavelength gratings," *J. Lightw. Technol.*, vol. 43, no. 6, pp. 2706–2715, Mar. 2025, doi: 10.1109/jlt.2024.3507941.
[30] H. Sun, Y. Wang, and L. R. Chen, "Integrated discretely tunable optical delay line based on step-chirped subwavelength grating waveguide Bragg gratings," *J. Lightw. Technol.*, vol. 38, no. 19, pp. 5551–5560, Aug. 18, 2020, doi: 10.1109/JLT.2020.3017496.
[31] Y. Li, L. Xu, D. Wang, Q. Huang, C. Zhang, and X. Zhang, "Large group delay and low loss optical delay line based on chirped waveguide Bragg gratings," *Opt. Exp.*, vol. 31, no. 3, pp. 4630–4638, Jan. 2023, doi: 10.1364/oe.480375.

HONG GAO received the B.S. degree in microelectronics science and engineering from China Jiliang University, China, in 2020. She is currently pursuing the M.S. degree in microelectronics and solid-state electronics with the Institute of Microelectronics, Chinese Academy of Sciences, China. Her research interest includes silicon photonics integration technology.

FUJUN SUN received the Ph.D. degree from Beijing University of Posts and Telecommunications, Beijing, China, in 2020. She is currently an Associate Professor with the Institute of Microelectronics, Chinese Academy of Sciences. Her current research interests include silicon photonics, nanophotonics, and optical microcavity.

GANG YANG received the M.Phil. degree from The University of Sydney, Australia, in 2021. He is currently an Assistant Engineer with the Institute of Microelectronics, Chinese Academy of Sciences. His current research interests include heterogeneous silicon photonics and photonic integrated circuits.

TIANYANG FU received the Ph.D. degree from Beijing University of Posts and Telecommunications, in 2024. She is currently a Postdoctoral Researcher with the Institute of Microelectronics, Chinese Academy of Sciences. Her research interests include silicon photonics devices and inverse design.

ZAILI YANG received the B.S. degree in electronic science and technology from Shandong University, China, in 2021. He is currently pursuing the Ph.D. degree in microelectronics and solid-state electronics with the Institute of Microelectronics, Chinese Academy of Sciences, China. His research interest includes programmable integrate photonics.

JING XIAO received the B.S. degree in optoelectronic information science and engineering from Beijing Jiaotong University, China, in 2022. He is currently pursuing the Ph.D. degree in microelectronics and solid-state electronics with the Institute of Microelectronics, Chinese Academy of Sciences, China. His research interests include silicon photonics integration technology and semiconductor quantum computing.

WEI TANG received the bachelor's degree in microelectronic science and engineering from Xiangtan University, in 2023. He is currently pursuing the master's degree in microelectronics and solid-state electronics with the Institute of Microelectronics, Chinese Academy of Sciences. His current research interests include silicon-based photonics, mainly including modulators and couplers.

YAN YANG received the Ph.D. degree from Nanyang Technological University, in 2016. She is currently a Professor with the Institute of Microelectronics, Chinese Academy of Sciences. Her research interests include silicon photonics and electronic-photonic integration.